View metadata, citation and similar papers at core.ac.uk

brought to you by CORE

provided by Analisis Harga Pokok Produksi Rumah Pada

Journal of Physics: Conference Series

PAPER • **OPEN ACCESS**

Naturalcarbon-metal composite for supercapacitor application

To cite this article: R Taslim *et al* 2018 *J. Phys.: Conf. Ser.* **1120** 012008

View the article online for updates and enhancements.

IOP ebooks™

Bringing you innovative digital publishing with leading voices to create your essential collection of books in STEM research.

Start exploring the collection - download the first chapter of every title for free.

This content was downloaded from IP address 114.125.56.108 on 02/01/2019 at 22:08

Naturalcarbon-metal composite for supercapacitor application

R Taslim[1*], A Agustino[2] and E Taer[2]

[1]Department of Industrial Engineering, State Islamic University of Sultan Syarif Kasim 28293 Simpang Baru, Riau, Indonesia.
[2]Department of Physics, University of Riau, 28293, Simpang Baru, Riau, Indonesia

[*]E-mail: rikataslim@gmail.com

Abstract. Water hyacinth (eichhornia crassipes)has been used as the material to produce carbon and metal oxide composite for supercapacitor electrode. The study focus on the effect of electrode thickness variation: (i) 0,26 mm (ii) 0.28 mm, and (iii) 0.30 mm on the electrode density and specific capacitance of the supercapacitor cell. The composite electrode was labeled as CMWH1, CMWH2, and CMWH3. The density of CMWHs electrode are 0.65 gcm^{-3}, 0.66 gcm^{-3}, and 0.70 gcm^{-3} for CMWH1, CMWH2, and CMWH3 sample respectively. These results show the density is directly proportional to the thickness of the electrode. Electrochemical properties characterization of CMWH electrode was performed using cyclic voltammetry method. The specific capacitance of the CMWH electrode is obtained at 97.64 Fg^{-1}, 108.43 Fg^{-1}, and 96.54 Fg^{-1} for CMWH 1, CMWH2 and CMWH3. Specific capacitance shows the optimum condition at 0.28 mm thickness. The difference trend of specific capacitance with density influenced by pseudocapacitance material properties that exist CMWH electrode. For addition, the TG Analysis, SEM, EDX, and XRD also included in the study.

1. Introduction

Supercapacitor or Electrochemical Double Layer Capacitor (EDLC) is an energy storage device other than the capacitor, battery and fuel cell [1]. Based on its energy storage mechanism, the supercapacitor is divided into two type: the electrochemical double layer capacitor (EDLC) and pseudocapacitor [2]. The EDLC works based on the formation of ions and electrons pairs at the boundary of electrolyte and electrode. The Electrodes commonly used in EDLC systems is the conductor material with a high surface area such as carbon, while pseudocapacitor works based on oxidation and reduction reactions that appear on certain materials such as metal oxides and conducting polymers. The carbon materials have advantages such as stable in physical and chemical properties, easily controlled pore properties and relatively low production costs [3,4], but produce cells with relatively low capacitance. The pseudocapacitor material has the advantage of high cell capacitance but with relatively high production cost. An alternative to improving supercapacitor cell performance but with low production costs can be developed with a combination of EDLC and pseudocapacitor systems. This combination of working principles can be made by producing carbon composite electrodes and pseudo materials or by preparing EDLC and pseudocapacitance hybrid cell materials. The carbon composite electrodes and material pseudo are a sufficiently effective way to reduce production costs but show good cell

Content from this work may be used under the terms of the Creative Commons Attribution 3.0 licence. Any further distribution of this work must maintain attribution to the author(s) and the title of the work, journal citation and DOI.
Published under licence by IOP Publishing Ltd

performance. The usual ways of developing composite electrodes are by mixing carbon and pseudo materials such as metal oxides or conduction polymers with the addition of adhesives material. Another common way to use is to grow metal oxide materials in nanostructures on the surface of carbon materials in a variety of shapes and sizes. Metal oxide materials are synthesized from artificial precursors so that production costs are still relatively high. The most commonly used metal oxides are manganese oxide [5], ruthenium oxide [6], nickel oxide [7,8], and cobalt oxide [9,10,11,12].

In this study, the composite electrode of carbon and metal oxide material is made from a natural organic material which naturally contains certain types of metals. The composite electrodes are synthesized from water plants that are easy to absorb some types of metal materials. Water hyacinth is selected as a natural medium that is usually able to absorb several types of metals such as Pb, Cd, Cu, Ni, and Zn [13]. However, the percentage of metal content that can be absorbed by these plants is relatively small so that in the synthesis of composite carbon electrodes, the carbon content of the electrode must be minimized. The focus of this study is to examine the nature of carbon composites and existing metal materials naturally in water hyacinth plants by varying the thickness of the electrodes. The carbon electrodes are produced in pellet form without additional adhesive to maintain the natural conductive properties of carbon materials. In this study electrode shaped pellets with a thickness of 0.26 mm has been able to show the nature of pseudocapacitance. Thus, this study has demonstrated the production of composite electrodes for a combination of EDLC and pseudo material principles through the synthesis of naturally available materials. These results can certainly improve the performance of supercapacitors and reduce production costs.

2. Experimental method

2.1 Preparation of activated carbon

The main material used in this study is water hyacinth. This raw material has been collected then washed to remove any dirt or mud, followed bysun-dried for 48 hours to reduce the moisture content in the sample. After the drying process, water hyacinth is cut into 3 cm in size, then oven-dried at a temperature of 110 °C for 48 hours. The next process is pre-carbonization carried out using the oven at a temperature of 250 °C for 2.5 hours [14,15]. Then, the sample was milled using ball milling for 20 hours in order to obtain sample sizeless than38 μm. The sample was then chemically activated using KOH activator at concentration 0.2 M. The KOH activators have been used in the study that we have reported previously [14,16,17,18,19]. The activated sample was molded to pellet form at a diameter of 19 mm using the Hydraulic press at 8 tons [15,20]. The carbonization process is carried out at a temperature of 600 °C in the N_2 gas environment [15,19,21,22] and followed by physical activation using CO_2 gas at a temperature of 850 °C for 2 hours. This physical activation time was in accordance with the activation time that we reported previously [14,19,23,24].All activated carbon samples are polished to the desired thickness and washed until the washing water becomes neutral.

2.2 Manufacture of supercapacitor cells

A pair of activated carbon pellets made from water hyacinth is used as electrodes in the manufacture of sandwich-shaped supercapacitor cells. Another material used is a pair of 316L stainless steel tape as a current collector, a duck eggshell membrane is used as a separator and 1 M sulfuric acid solution is used as the electrolyte. The carbon electrodes were immersed using 1 M H_2SO_4 electrolyte solution for 48 hours, then assembled into supercapacitor cells as we previously reported [16,20,21].

2.3 Characterization of carbon electrodes

The physical properties tested on carbon electrode from water hyacinth include thermal properties, density, surface morphology, elemental content and crystalline degree. The thermal properties test is performed using the Thermogravimetric Analysis (TGA) method. The TGA testing was performed in an N_2 gas environment to a temperature of 600 °C at a temperature scan rate of 10 °C min^{-1} using Netzsch derivatograph (STA 449 F1 Jupiter instrument). The density of carbon electrodes is obtained from measurements of mass, diameter, and thickness of each sample before and after the

carbonization-activation process is carried out. The activated carbon electrode varied for three different thickness by the polished process. The N_2 gas adsorption-desorption testing was carried out using the Brunauer Emmet Teller method using Quantachrome Instruments version 11.0 for analysis of the specific surface area of carbon electrode sample. Morphological structure testing and element content were carried out using Scanning Electron Microscopy and energy dispersive X-ray using JEOL-JSM 6510 LA instrument. The X-ray diffraction test was used to determine the lattice and crystalline phase parameters in carbon samples using X-pert powder panalytical diffractometer with CuKα ray source, with a wavelength of 0.154 nm and the diffraction angle used was 2θ ie at an angle range of 10-100°.

2.4Electrochemical properties

The measurement of electrochemical properties of supercapacitor cells was performed using Cyclic Voltammetry (CV) method. This measurement uses the Physics CV UR Rad-Er 5841 and calibrated with VersaStat II Princeton Applied Research calibrator standard instrument. This measurement was carried out at a potential window range of 0 V-0.5 V and a scan rate of 1 mVs^{-1}[18,22,25]. The specific capacitance (C_{sp}) was calculated usingthe following equation:

$$C_{sp} = \frac{I_c - I_d}{Sxm} \quad (1)$$

Where I_c is the charging current (A), I_d is the discharge current (A), S is the scan rate and m is the mass of the electrode.

3. Results and Discussion

3.1 Thermogravimetry analysis

Thermal properties were analyzed by Thermogravimetric (TG) and Differential Thermal Termographymetry (DTG). The parameters studied was changes in the sample mass to the temperature change. The DTGis used to measure test for the rate of change in sample mass against temperature rise. Both of these analyzes were carried out at a temperature range of 30-600 °C at a heating rate of 10 °C min^{-1} in the N_2 gas environment. The mass of sample for thermal analysis is7.199 mg. The thermal properties data for pre-carbonize water hyacinth samples isshown in Figure 1.

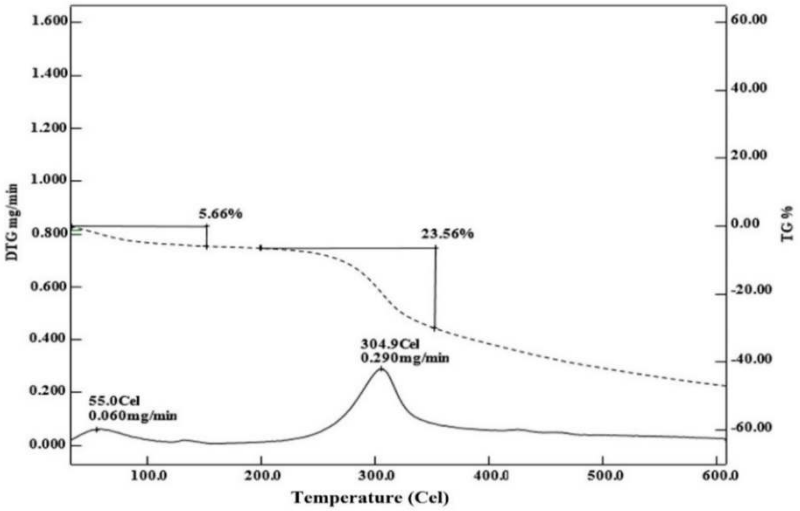

Figure 1. The TG, and DTG profile curves for water hyacinth samples

Figure 1 shows the profile of the sample mass change in the percent (%) to the temperature (C). The TG curve of Figure 1 was represented by dashed line. The TG data shows the pattern of sample mass reduction when the temperature is raised. Significant mass reductions occurred in the temperature range of 30-151 °C, 210-353 °C and subsequently the sample mass decreased gradually from a temperature of 353-600 °C. The first mass reduction in the first temperature range of 30-151 °C as high as 5.66% affected by the release of water content [26,27,28]. The second one at a temperature range of 210-353 °C amount 23.56% is influenced by the simultaneous decomposition of cellulose and hemicellulose [29], whereas in the third stages the sample mass reduction occurs due to lignin decomposition [30,31].

The DTG curve is indicated by the solid line in Figure 1, the shape of the curve is marked by the presence of two peaks at temperatures of 55 °C and 304.9 °C, respectively. This peak shows in the optimum mass reduction rate to the temperature. The first peak shows the optimum mass degradation rate in the temperature range 30 -151 °C by 0.060 mg min^{-1}, while at the second peak shows the optimum mass degradation rate experienced by the sample is 0.290 mg min^{-1} and occurs in the temperature range 210-353 °C. This temperature of 304.9 °C shows the optimum mass degradation rate which is the maximum decomposition of the basic elements of the sample to increase the carbon elements. This temperature is then chosen as the resistance temperature in the sample carbonization process to ensure a higher level of carbon purity.

3.2 Mass, diameter, thickness and density of theelectrode

The measurements results of mass, diameter, thickness, and density of the electrodes before and after carbonization-activation, and after the polishing process are shown in Table 1. The mass, diameter, thickness, and density of the electrode before the carbonization-activation process is almost the same, this result was reasonable because of the same sample treatment while the difference in result is due to the pre-carbon powder being wasted during the molding process at a compression pressure.The mass, diameter, thickness, and density of CMWH electrodes after the carbonization-activation process have decreased due to the release of non-carbon materials during the carbonization-activation process [32].The CMWH electrode mass after the polishing process shows a difference, this is due to the difference in electrode thickness, the greater electrode thickness will result in a higher electrode mass. While the diameter of the electrode after the polishing process also has a different, this is due to electrode erosion during polishing.The different in electrode density after polishing because of the difference in thickness for every sample. The highest density was found by the CMWH3 sample with an electrode thickness of 0.30 mm which is 0.70 gcm^{-3}, while the smallest density value is CMWH1 sample with a thickness of 0.26 mm which is 0.65 gcm^{-3}. This result is influenced by changes in mass and diameter due to the polishing process.

Tabel 1. Mass (g), diameter (mm), thicness (mm), and density (gcm^{-3})

Sample codes	Before carbonization-activation				After carbonization-activation				After polishing			
	m	d	t	ρ	M	d	t	ρ	M	d	t	ρ
CMWH1	0.582	19.72	0.235	0.81	0.192	13.58	0.162	0.82	0.022	12.90	0.26	0.65
CMWH2	0.59	19.95	0.243	0.78	0.195	13.85	0.161	0.80	0.0235	12.68	0.28	0.66
CMWH3	0.573	19.78	0.234	0.80	0.213	14.29	0.168	0.79	0.028	13.01	0.30	0.70

3.3 N_2 gas adsorption-desorption isothermsAnalysis

Figure 2a shows the N_2 gas adsorption-desorption isotherm data on the carbon electrodes sample, this data shows the relationship between the adsorption-desorption volume to the relative pressure (P/P_0). The N_2 gas adsorption-desorption model shown in Figure 2a was type IV according to the IUPAC classification although there is a slight difference in the relatively large pressure conditions. The assertion of type IV is shown by an increase in absorption volume at a relative pressure of 0.4.

Figure 2b shows the relationship between dV/dr (d) to the sample pore diameter using the BJH method. The BJH method was used to see the pore distribution from the range of 3.5 to 40 nm. It can be seen that the decrease in pore volume occurs in the pore diameter range of 3.5-7.0 nm and shows the maximum pore volume at 3.5 nm diameter of 0.001 $cm^3nm^{-1}g^{-1}$. The maximum absorption volume shows that the dominant sample pore diameter is in the range mesoporous. The assertion of type IV adsorption-desorption data is strengthened with an average of BJH pore diameter of 3.5911 nm, which shows the average pore diameter of the sample was in the mesoporous group corresponding to type IV characteristics [33]. Senthilkumar et al. 2013 with the same material also obtained a pore diameter in the mesoporous range [33].

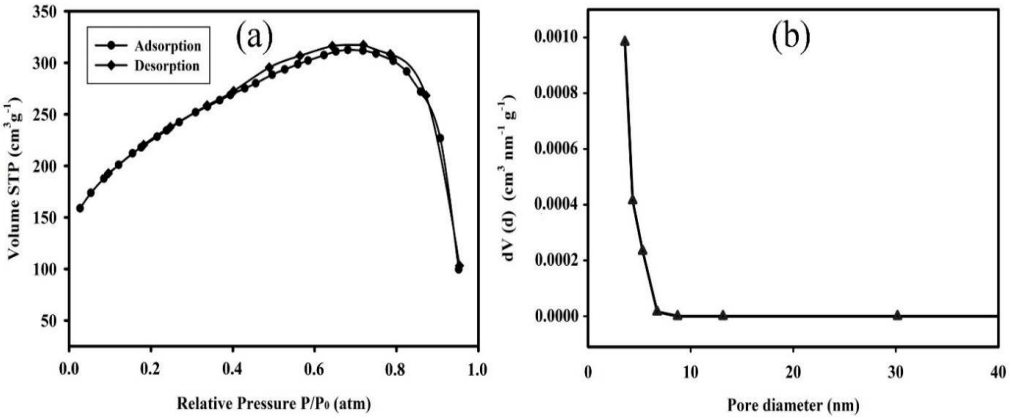

Figure 2. (a) N_2 gas adsorption-desorption isotherm and (b) pore size distributions

The specific surface area data (S_{BET}), BJH surface area, BJH volume, and diameter are shown in Table 2. Zhang et al, 2012 and Kurniawan et al, 2015 also studying the same material obtained specific surface area (S_{BET}) of 579.94 m^2g^{-1} [34] and 761 m^2g^{-1} [35].

Table 2. The N_2 gas absorption measurements result from CMWH sample

Sample	S_{BET} (m^2g^{-1})	S_{BJH} (m^2 g^{-1})	V_{BJH} (cm^3 g^{-1})	D_{BJH} (Å)
CMWH	776.213	130.548	0.133	35.911

3.4 Scanning electron microscopy analysis

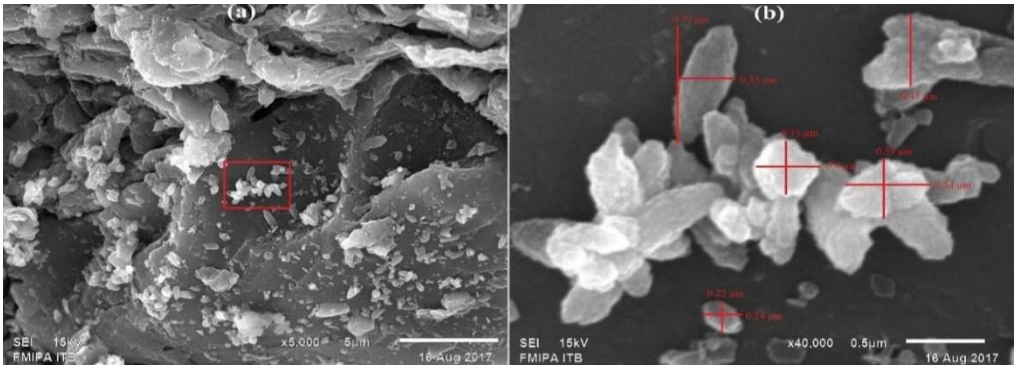

Figure 3. The SEM micrograph of CMWH sample (a) CMWH at magnification 5000x (b) CMWH at 40000x magnification

Figures 3a and 3b show the SEM micrograph CMWH sample at 5000x and 40000x magnification.Figure 3a with a shows the surface morphology of CMWH which is shaped like a lump

and is dominated by black color which is assosiated with carbon particle and also seen particles that are smooth white indicating other elements than carbon. At this magnification, there is also no macropore on the surface of the CMWH sample. While Figure 3b is an enlargement in the area marked in red in Figure 3a. These smooth particles have a shape that tends to be regular with an oval shape dominated by a length of 0.44 μm and 0.38 μm wide.

3.5 Energy dispersive x-ray analysis

The EDX test results of the sample are shown in Figure 4 which were selected in an area of 15 μm^2 which is indicated by a green box in the SEM image that is inserted in the upper right side. The EDX data shows the elements contained in CMWH samples namely carbon (C), magnesium (Mg), potassium (K), calcium (Ca), manganese (Mn), copper (Cu), strontium (Sr) and barium (Ba). The content of the constituent elements of the sample is dominated by carbon and calcium at 0.277 keV and 3.690 keV indicated by the highest count, respectively. The mass and atomic percentage were 69.74%, 88.55%, for carbon and 24.44%, 9.30% for calcium, respectively. The other elements such as Magnesium, potassium, manganese, copper, strontium, and barium with energies of 1.253 keV, 3.312 keV, 5.894 keV, 8.040 keV, 1.806 keV and 4.464 keV, respectively. The other studies with the same raw material also found the presence of other elements than carbon such as chlorine, potassium, oxygen, and calcium [27].The complete data on the elements contained in the sample are shown in Table 3.

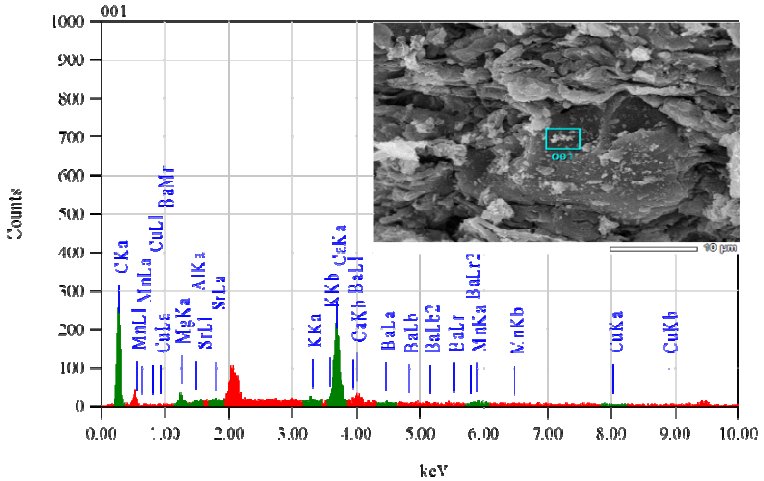

Figure 4. The Energy dispersive X-rays measurement result data of CMWH samples

Table 3. Percentage of elements contained in the CMWH electrode

No	Elements	mass (%)	atom (%)
1	Carbon (C)	69.74	88.55
2	Magnesium (Mg)	1.60	1.01
3	Pottasium (K)	0.72	0.28
4	Calsium (Ca)	24.44	9.30
5	Mangan (Mn)	2.31	0.64
6	Copper (Cu)	0.36	0.09
7	Strontium (Sr)	0.78	0.14
8	Barium (Ba)	0.05	0.01
	Total	100	100

3.6 X-ray diffraction analysis

The curve of X-ray diffraction characterization results for CMWH sample can be seen in Figure 5. The XRD diffractogram data shows the relationship between X-ray intensity (a.u) and scattering angle of 2θ (degrees), this data shows that there are two broadening peaks at 2θ angles of 24.429° and 46.198°, which correspond to the scattering plane of d_{002} and d_{100} for carbon materials [36].In Figure 5a these two peaks are not very clear, especially the peak corresponds to the angle of 24.429°, after going through the process of normalization using the Microcal origin software these two peaks look more clearly and are shown in Figure 5b. Both of these broadening peaks indicate the CMWH sample has an amorphous structure. The angle 2θ illustrates the distance between the lattice layers (d_{hkl}) which is affected by the structure of the particle, where the greater of the scattering angle 2θ the smaller the resulting d_{hkl}. The CMWH sample has d_{hkl} for planes d_{002} and d_{100}, respectively 3.64 Å and 1.96 Å. The stack height (L_c) as high as 9.41 Å and stack width (L_a) of 8.01 Å. In addition also found some sharp peaks and are marked with an asterisk at an angles of 23.02°; 29.36°; 31.91°; 35.95°; 37.5°; 39.38°; 43.12°; 47.44°; 53.81°; 56.56°; 57.35°; 60.65° and 65.52°. This sharp peak indicates the presence of Calcium carbonate ($CaCO_3$) and Cellulose ($C_6H_{10}O_5$) compounds. The presence of Calcium carbonate and Cellulose compounds in the CMWH sample is derived from materials absorbed from the environment and the constituent materials for water hyacinth plants.

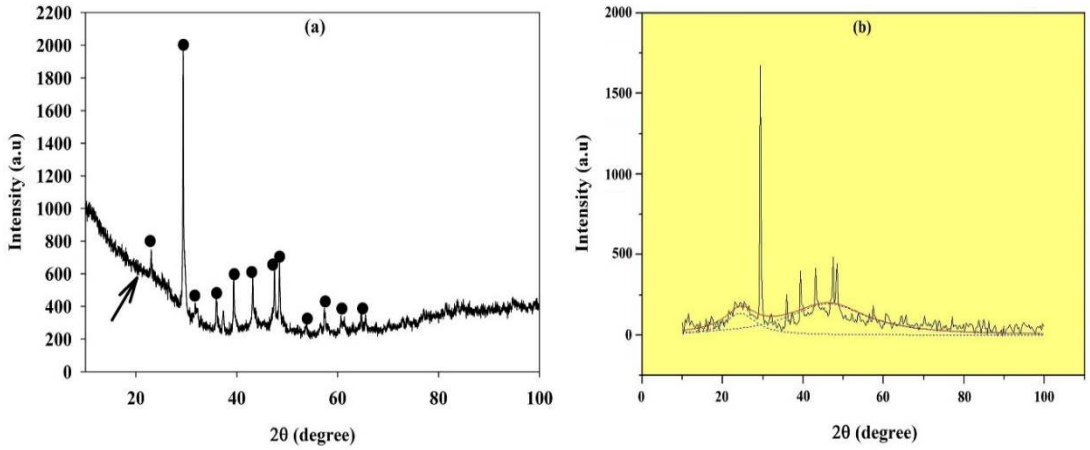

Figure 5. (a) CMWH sample X-ray diffraction pattern, (b) Fittings using microcal origin software

3.7 Cyclic Voltammetry (CV) Analysis

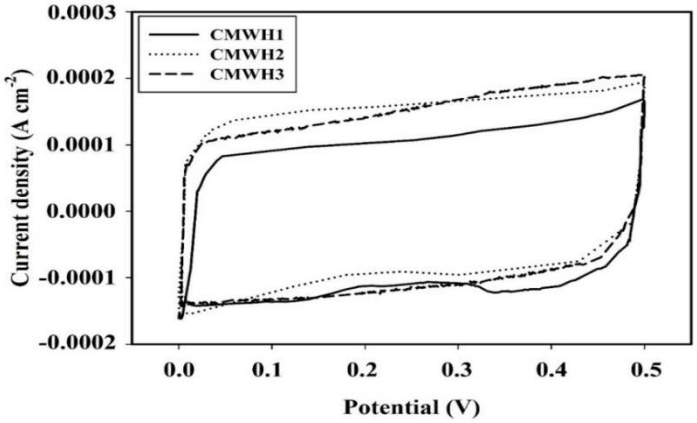

Figure 6. The CV curve of supercapacitor cell for CMWH1, CMWH2, and CMWH3 samples

Figure 6 shows Cyclic Voltammetry (CV) data CMWH electrode in the voltage range of 0 to 0.5 Volt with a scan rate of 1 mVs^{-1}. The CV curve shows the relationship between current density (Acm^{-2}) to the voltage (Volt). The CV curve has almost like a rectangular shape, and there is an increase in the current density at a potential of 0.4 V during the discharge process for CMWH1 and CMWH2 samples. The appearance of the current increase which almost resembles the peaks in CMWH1 and CMWH2 samples are indicated by an oxidation reaction which releases a little more ions. The increasing current in both samples was due to its having a smaller thickness than the CMWH3 sample. The redox reaction doesn't appear on the CMWH3 electrode because of the higher thickness the pseudocapacitive effect covered by a double layer mechanism. The results of other studies with the same material also obtained the presence of pseudocapacitive properties given by redox reactions and occur in oxygen and nitrogen functional groups [37,38].

The electrode properties such as thickness (t), mass (m), scan rate (S), current charge (I_c), Current discharge (I_d) and Specific capacitance (C_{sp}) for three electrode samples are shown in Table 4.

Table 4. The electrode thickness (t), mass (m), scan rate (S), charge current (I_c), discharge current (I_d) and Specific capacitance (C_{sp}) of three electrode samples

Sample codes	t (mm)	m (g)	S (Vs^{-1})	I_c (A)	I_d (A)	C_{sp} (Fg^{-1})
CMWH1	0.26	0.022	0.001	0.001069	-0.001079	97.64
CMWH2	0.28	0.0235	0.001	0.001389	-0.001159	108.43
CMWH3	0.30	0.028	0.001	0.001550	-0.001153	96.54

Based on the data in Table 4 the highest to the lowest specific capacitance of supercapacitor cells were 108.43 Fg^{-1}, 97.64 Fg^{-1} and 96.54 Fg^{-1} for CMWH2, CMWH1 and CMWH3 electrodes, respectively.The specific capacitance is affected by the magnitude of the charge and discharges current obtained from the CV measurement. So that, the higher the charge and discharge current was obtained then the higher electrode specific capacitance.

Table 5 shows the comparison of the specific capacitance of supercapacitor electrodes from water hyacinth with the different production methods. Based on Table 5, carbon electrode from water hyacinth waste indicates good potential for use as carbon electrodes in supercapacitor devices, however has relatively lower capacitive properties.

Table 5. Comparison of the specific capacitance of supercapacitor electrodes from water hyacinth

Materials	Method	C_{sp} (Fg^{-1})	References
Water hyacinth	$ZnCl_2$ activation at di□erent carbonization temperatures (500, 600, 700, 800 and 900 ^oC)	472	[34]
Water hyacinth	Subcritical water hydrolysis and carbonization methods	179.6	[35]
Water hyacinth	pre-carbonization and KOH activation	344.9	[38]
Water hyacinth	large porous sheet-like carbon materials	273	[39]
Water hyacinth	Activated carbon monolit, pre-carbonization, KOH activation, CO_2 activation	108.43	present study

4. Conclusion

Based on all data analysis it can be concluded that water hyacinth as a promising raw material for the production of carbon and metal oxide composites without addition of adhesive material as electrodes on supercapacitor devices. The thickness of the electrode affects the electrode density, its effect on the combination mechanism EDLC and pseudocapacitance to find the optimum specific capacitance. The optimum specific capacitance of supercapacitor cells as highs as 108.43 Fg^{-1} with electrode thickness of 0.28 mm.

Acknowledgements

We would like to thank the Rector of the State Islamic University of Sultan Syarif Kasim Riau for the finansial support by using the basic cluster of scientific integration 2018 with the Principal researcher of Dr. Rika, S.Si., M.Sc with the project titled "Utilization of aquatic weed plants as the raw material for the production of supercapacitor electrodes" with contract number: 0935/R/2018.

References

[1] Burke A 2000*J. Power Sources*9137
[2] ZhangY, Feng H, Wu X, Wang L, Zhang A, Xia T, Dong H, Li X and Zhang L 2009 *Int. J. Hydrogen Energy*344889
[3] Pandolfo A G and Hollenkamp A F 2006*J. Power Sources*157 11
[4] Frackowiak E and Beguin F 2001 *Carbon*39 937
[5] Huang Q, Wang X. and Li J 2006*Electrochim. Acta*52 1758
[6] Mondal S K and Munichandraiah N 2008*J. Power Sources*175 657
[7] Cheng J, Cao G P and Yang Y S 2006*J. Power Sources*159 734
[8] Xu J, Gu X, Cao J, Wang W and Chen Z 2012*J. Solid State Electrochem.*162667
[9] Svegl F, Orel B, Hutchins M G and Kalcher K 1996*J. Electrochem. Soc.*143 1532
[10] Wei T Y, Chen C H, Chang K H, Lu S Y and Hu C C 2009*Chem. Mater*. 21 3228
[11] Li Y, Huang K, Yao Z, Liu S and Qing X 2011*Electrochim. Acta*56 2140
[12] Ali M A G, Fouad A O, Makhlouf A S and Chongm F K 2014*J. Solid State Electrochem.*182505
[13] Mahmood T, Malik S A and Hussain S T 2010*Bioresour.*51244
[14] Taer E, Susanti Y, Awitdrus, Sugianto, Taslim R, Setiadi R N, Bahri S, Agustino, Dewi P, and Kurniasih B 2018*AIP Conf. Proc.*1927030016-1
[15] Taer E, Dewi P, Sugianto, Syech R, Taslim R, Salomo, Susanti Y, Purnama A, Apriwandi, Agustino and Setiadi R N 2018 *AIP Conf. Proc.*1927 030026-1
[16] Farma R,Deraman M, Omar R, Awitdrus, Ishak M M, Taer E, and Talib I A 2011. *AIP Conf. Proc*. 1415 180
[17] Taer E, Iwantono, Manik S T, Taslim R, Dahlan D, and Deraman M 2014*Adv. Mater. Res.*896179
[18] Taer E, Mustika W S, Agustino, Fajarini, Hidayu N. and Taslim R 2017 *IOP Conf. Ser.: Earth Environ. Sci.*58 012065
[19] Taer E, Kurniasih B, Sari F P, Zulkifli, Taslim R, Sugianto, Purnama A, Apriwandi and Susanti Y 2018*AIP Conf. Proc.*1927 030006-1
[20] Taer E,Deraman M,Talib I A,Umar A A,Oyama M and Yunus R M 2010*Curr. Appl. Phys.*10 1071
[21] Taer E, Sugianto, Sumantre M A,Taslim R, Iwantono, Dahlan D, and Deraman M 2014*Adv. Mater. Res.* 89666
[22] Taer E, Apriwandi, Yusriwandi, Mustika W S, Zulkifli, Taslim R, Sugianto, Kurniasih B, Agustino and Dewi P 2018 *AIP Conf. Proc.* 1927 030036-1
[23] Taer E, Deraman M, Taslim R, and Iwantono 2013*AIP. Conf. Proc.* 1554 37
[24] Taer E, Taslim R, Mustika W S, Kurniasih B, Agustino, Afrianda A, and Apriwandi 2018*Int. J. Electrochem. Sci.*138428

[25] Taer E, Taslim R, Aini Z, Hartati S D and Mustika W S 2017 *AIP. Conf. Proc.*1801 040004-1
[26] Luo G, Strong J, Wang H, Ni W, Shi W 2011*Bioresour. Technol.*1026990
[27] Madrid J F, Nuesca G M and Abad L C 2013*Rad. Phys. Chem.*85 182
[28] Gao Y, Wang X, Wang J, Li X, Cheng J, Yang H and Chen H 2013*Energy*58 376
[29] Yao F, Wu Q, Lei Y, Guo W, Xu Y, 2008*Pol Deg. Stability*93 90
[30] Fisher T, Hajaligol M, Waymack B, Kellogg D 2002*J. Anal. Appl. Pyrol.*62 331
[31] Harun M Y, Radiah A B D, Abidin Z Z and Yunus R 2011*Bioresour. Technol.*102 5193
[32] Farma R, Deraman M, Awitdrus, Talib I A, Omar R, Manjunatha J G, Ishak M M, Basri N H, and Dolah B N M 2013*Int. J. Electrochem. Sci.*8 257
[33] Senthilkumar S T, Selvan R K, Lee Y S and Melo J S 2013 *J. Mater. Chem. A*1 1086
[34] Zhang X, Wang X, Su J, Wang X, Jiang L, Wu H and Wu C 2012 *J. Power Sources*199 402
[35] Kurniawan F, Wongso M, Ayucitra A, Soetaredjo F E, Angkawijaya A E, Ju Y -H and Ismadji S 2015*J. Taiwan Inst.Chem. E.*47 197
[36] Taer E, Deraman M, Thalib I A, Awitdrus A, Hasmi S A, Umar A A 2011*Int. Journal Electrochem. Sci.*6 3301
[37] Huang C W, WuY T, Hu C C and LiY Y2007*J. Power Sources*172 460
[38] Zheng K, Li Y, Zhu M, Yu X, Zhang M and Cheng J 2017*J. Power Sources*366 270
[39] Wu X, Hong X, Luo Z, Hui K S, Chen H, Wu J, Hui K N, Li L, Nan J, Zhang Q 2013*Electrochim. Acta*89 400